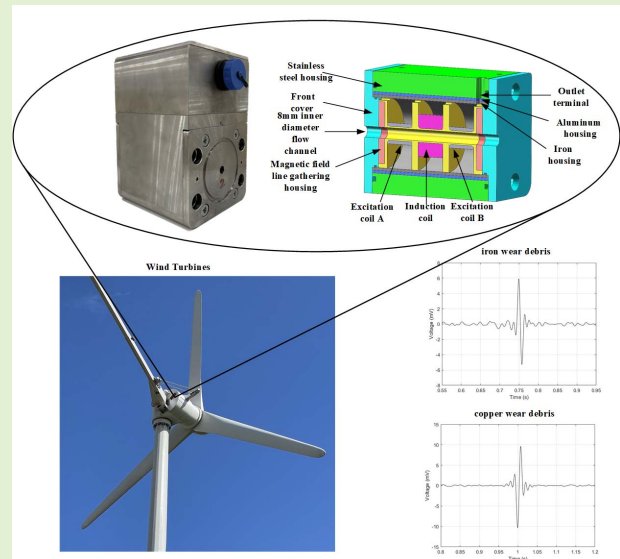


# Online Symmetric Magnetic Excitation Monitoring Sensor for Metal Wear Debris

Kai Li<sup>1</sup>, Member, IEEE, Wenbin Bai, Yuan Li<sup>1</sup>, Shichao Zhou, and Peng Wen

**Abstract**—The metal wear debris in mechanical transmission can feedback the characteristics of mechanical equipment failure, and its online monitoring efficacy directly affects the operating performance of mechanical equipment. Specific to the need for online fault detection of the mechanical transmission system, a double-coil reverse excitation method is adopted to provide a magnetic field environment for metal wear debris testing in the lubricating oil circuit of the mechanical transmission system. Based on the magnetic field distribution model of a single-coil solenoids, a coupling magnetic field distribution model of reverse-symmetric double-coil magnetic excitation is established. On the basis of detecting the coils to obtain the signals of magnetic field disturbance when metal wear debris passing through the magnetic excitation field, an online monitoring sensor for metal wear debris with a reverse-symmetric double-coil magnetic excitation balance magnetic field is developed. Taking the monitoring of metal wear debris in a large-aperture flow channel as an example, a semi-physical simulation test has been carried out on metal wear debris in different grain diameters and textures, whose experimental results indicate that this sensor can detect 100  $\mu\text{m}$  ferromagnetic metal and 1000  $\mu\text{m}$  non-ferromagnetic metal in an 8 mm flow channel, which, as a detection sensor for metal wear debris, can also be used for metal wear debris monitoring in the mechanical lubricants of mechanical transmission and engines.

**Index Terms**—Metal wear debris, electromagnetic induction, symmetric magnetic excitation, electromagnetic detection.



## I. INTRODUCTION

IN ORDER to accurately control the operation of mechanical equipment in the sectors of modern industry, civilian use, and military science, hydraulic systems, and lubrication systems have been widely used in mechanical automation and other fields, which has the increasing demand for online fault diagnosis of mechanical equipment during operation. During the operation of mechanical equipment, wear debris are generated due to mutual friction, collision, and intrusion of pollutants [1], and its online and offline detection is not only an important means to judge the wear conditions of

mechanical equipment but also an important basis for predicting equipment service life and fault detection [2], [3], which has become an important research direction for failure monitoring of mechanical equipment.

Oil detection sensors can be divided into optical [4], ultrasonic [5], capacitive [6], [7], and inductive sensors, of which the optical sensor has high detection sensitivity, but is easily affected by the oil transmittance [8], the ultrasonic sensor can distinguish solid particles and air bubbles in the oil, but unable to distinguish the magnetic properties of metal particles [9], the capacitive sensor can detect water droplets and bubbles in the oil, but unable to distinguish the types of metal wear debris [10]. Since the magnetic field disturbance generated when metal wear debris pass through the oil circuit has the better properties of metal category characterization, the inductance detection method has been given a high priority in the field of metal wear debris detection. However, the online metal wear debris monitoring technology suitable for the application in the industrial field has been a major technical challenge in terms of the demands for online detection and online failure prediction since the magnetic field disturbance

Manuscript received January 2, 2022; accepted January 17, 2022. Date of publication January 19, 2022; date of current version March 14, 2022. This work was supported in part by the Natural Science Foundation of Shanxi Province, China, under Grant 201901D211251 and Grant 20210302123058. The associate editor coordinating the review of this article and approving it for publication was Dr. Mert Torunbalci. (Corresponding author: Kai Li.)

The authors are with the School of Information and Communication Engineering, North University of China, Taiyuan 030051, China (e-mail: likai@nuc.edu.cn; s1905009@st.nuc.edu.cn; liyuan82@nuc.edu.cn; s2005021@st.nuc.edu.cn; s2005057@st.nuc.edu.cn).

Digital Object Identifier 10.1109/JSEN.2022.3144745

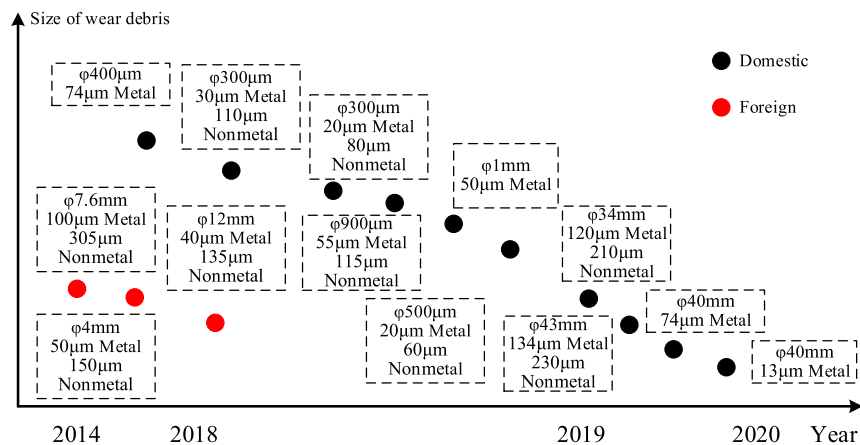


Fig. 1. Development process of metal wear debris detection technology.

signal generated by the metal wear debris is relatively weak compared to that from the environmental magnetic field, and its signal-to-noise ratio is relatively small.

In the early days, the inductive detection method was mainly used in terms of the research on detection technology of metal wear debris in the industrial field. At present, the MetalSCAN sensor developed by GasTOPS, a Canada-based company, can detect 100  $\mu\text{m}$  metallic wear debris and 250  $\mu\text{m}$  non-metallic wear debris in a 7.6 mm flow channel [11], and FG-on-line metallic wear debris sensor developed by Kittiwake, a UK-based company, can detect the ferromagnetic wear debris with the size larger than 40  $\mu\text{m}$  and the non-ferromagnetic metal wear debris with the size larger than 135  $\mu\text{m}$  in a 12 mm flow channel [12].

At this stage, electromagnetic induction technology plays an important role in the detection of metal wear debris in micro-channel and large-flow pipe diameters. At present, this electromagnetic induction sensor technology has mainly consisted of structural design technology and circuit compensation technology. The structural design mainly includes the optimal structural parameter design of the sensor [13], [14], the design of detection structures such as one-excitation and multi-induction and multi-excitation and one-induction new sensors, the structure design of capacitive and inductance detection modes [15], and the structure design of the internal magnetic field enhancement of the sensor, etc. Circuit compensation technology mainly includes resonance circuit, phase-division multiplexing circuit, asymmetrical compensation circuit for excitation coils [16] and so on.

Aiming at the microfluidic inductive sensor, Bai *et al.* [17] increased the magnetic field intensity by filling the sensor with superparamagnetic materials, thereby increasing the signal-to-noise ratio of particle detection. In order to improve the throughput of the microfluidic sensor, Liu's team [18] built the dual-channel detection systems based on the principle of phase-division multiplexing that reached the effect to detect 74-88  $\mu\text{m}$  iron wear debris. On account of the resistance detection method that is more sensitive to the detection of non-ferromagnetic particles, Ma *et al.* [19] proposed an inductance-resistance microfluidic sensor based on a dual solenoid coil structure, which can improve the detection accuracy of copper

wear debris up to 60  $\mu\text{m}$  in a 500  $\mu\text{m}$  flow channel, effectively making up for the imperfection of inductive sensor's low detection ability for non-ferromagnetic particles. Later, a new structure combining a planar coil with a ferrite core was proposed [20], which increased the throughput while improving the signal-to-noise ratio. In order to realize the detection of multi-pollutants in micro-channels, based on the inductance and capacitance detection methods, Zhang's team proposed a multi-parameter measurement sensor, which adopted a structure with annular flow channel being vertically embedded with the inner hole of two fitted planar coils [21], [22] and then, the silicon steel sheet [23] was added to optimize the coils into a solenoid structure in order to improve the detection accuracy [24]. In the 300  $\mu\text{m}$  annular flow channel, 30  $\mu\text{m}$  iron particles, 110  $\mu\text{m}$  copper particles, 100  $\mu\text{m}$  water droplets and 180  $\mu\text{m}$  bubbles can be detected.

Currently, the major technical bottleneck of the inductive wear debris sensor lies in the detection accuracy of the sensor limited by the flow channel aperture. The micro-channel metal wear debris sensor can realize high-precision wear debris detection but cannot maintain high throughput, and the limitation of the flow channel aperture can reduce the flow rate of the lubricating oil, affect the operation of the equipment, possibly causing serious consequences such as blockage of the flow channel. The high-throughput sensor can perform the high-throughput metal abrasive detection of the lubricating oil circuit in a variety of mechanical equipment, which has a small effect on the flow rate of the lubricating oil and can effectively avoid blockage of the flow channel, but has the problems such as low detection accuracy.

The sensitivity of the sensor can be improved by circuit compensation technology, which means, when the coil is in the state of parallel resonance, it will amplify the change in the impedance of the coil caused by particles and enhance the induced electromotive force output by the sensor. Based on this principle, Du's team [25] designed a double-layer planar coil, which can actually detect 45  $\mu\text{m}$  iron wear debris and 125  $\mu\text{m}$  copper wear debris in a 1mm microfluidic channel, effectively improving the sensitivity for detection of signal-to-noise ratio.

During the innovative research on sensor structures, proper use of new excitation structures can expand the throughput

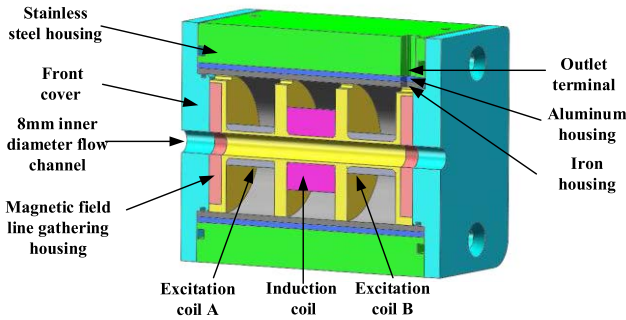


Fig. 2. The model of magnetic excitation detection structure with central weak disturbance.

of sensors while maintaining their accuracy. Zhu's team [26] proposed a sensor structure composed of  $3 \times 3$  sensing channels, which can realize the detection with 9 paths of sensor signals at the same time, and the sensitivity for the sensor to detect ferromagnetic wear debris can reach  $50 \mu\text{m}$  through a 1 mm aperture. In order to improve the detection accuracy of the high-throughput oil sensor, Ren *et al.* [27] adopted a new sensor probe with one-excitation and multi-induction to layout multiple induction coils in the flow channel for particle detection, which can identify the  $120 \mu\text{m}$  iron wear debris and  $210 \mu\text{m}$  non-ferrous wear debris in the 34 mm oil circuit, but this structure will reduce the flow rate of the lubricating fluid and fail to meet the requirements of actual working conditions. Xiao's team [28] proposed a local high-gradient magnetic field sensor that can detect  $13 \mu\text{m}$  ferromagnetic particles in a 40 mm aperture, but this sensor can only monitor the wear debris with a radial height of less than 8 mm in the flow channel, based on which Xiao's team [29] designed a new type of six-excitation structure inductive sensor to cover the 40 mm diameter flow channel, able to detect the sensitivity of  $13 \mu\text{m}$  ferromagnetic wear debris at full flow, but it did not mention non-ferromagnetic particle detection effect.

In order to solve the problem that the oil detection sensor cannot perform the monitoring on the full-flow high-sensitivity metal wear debris, a kind of magnetic excitation feedback information measuring sensor for metal wear debris in the large-aperture and high-flux oil is taken as the research object in this paper, that is, during the process when the metal wear debris passing through the large-aperture channel, by utilizing the symmetric characteristics of the excitation magnetic field area where the detection coil is located, enabling the excitation magnetic field detected by the detection coil is theoretically zero; under the condition that the effect of the primary magnetic field on the response magnetic field of the metal wear debris are avoided, the detection to magnetic field disturbance can be realized when the metal wear debris pass through the detection coil, while the adjustment module is used to adjust the magnetic field signals output by the detection coil, the signal feature processing module decomposes the magnetic field signal. Through an oil path experiment with aperture of 8mm and a maximum flow rate of 5.87 m/s, which has realized the effective detection of  $100 \mu\text{m}$  ferromagnetic wear debris and  $1000 \mu\text{m}$  non-ferromagnetic wear debris, and then the design of an online high-sensitivity sensor with metal wear

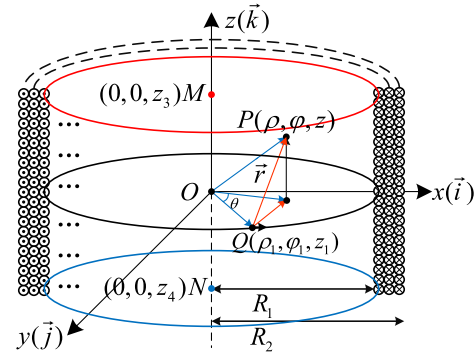


Fig. 3. Schematic diagram of magnetic field distribution inside single excitation coil.

debris passing through the main oil circuit with a large aperture along with the oil can be realized.

## II. DESIGN OF SENSOR

### A. Sensor Structure

The model of magnetic excitation detection structure with central weak disturbance is as shown in Fig. 2. The detection model adopts a symmetrical reverse double-coil structure and uses a magnetically inert material that is not affected by magnetic field energy as the skeleton of the coil [30]. It includes two sets of reverse winding excitation coils and one set of induction coils. The winding directions of the excitation coils can be divided into co-winding or reverse winding. Ideally, when the excitation coil is wound in the opposite direction, the two symmetric excitation coils are excited by the same excitation signal source, so that the alternating magnetic field generated by the excitation coil can be offset at the center of the structure; in the same way, when the excitation coil is wound in the same direction, it is only necessary to ensure that the phase difference of the excitation signal sources of the two excitation coils is  $180^\circ$  and the amplitude is consistent, and the magnetic field intensity at the midpoint of the interval between the two excitation coils can also be zero. The induction coil is located at the center of the two excitation coils. The three sets of coils are isolated by the skeleton, and the oil flows through the hollow tube inside the skeleton. When metal wear debris pass through the sensor, the zero magnetic field state of the center is disturbed, and the induction coil generates induced electromotive force. According to the magnitude and phase change of the induced electromotive force, the size and magnetic properties of metal wear debris can be determined. The change trend of induced electromotive force produced by ferromagnetic metal particles and non-ferromagnetic metal wear debris are opposite [31].

### B. Magnetic Excitation Model for Metal Wear Debris in Oil

When the sensor is in operation, the metal wear debris are enveloped in the oil and pass through the sensor, the signal output by the metal wear debris disturbs the magnetic field is affected by the internal magnetic field of the sensor. In order to analyze the relationship between the sensor signal output and

the internal magnetic field, a schematic diagram of the internal magnetic field distribution of the sensor is established.

In the current-carrying circular space with excitation radius  $\rho$  and excitation current  $I$ , the magnetic field distribution at arbitrary point is shown in Fig. 3. The schematic diagram uses a cylindrical coordinate system as the representation method. Taking the circular surface where the current-carrying ring is located as the  $Oxy$  plane, the center of the circle is the coordinate origin  $O$ , the axis direction of the solenoid is the  $z$  axis, the coordinate of the current-carrying element of the excitation coil is  $Q(\rho_1, \varphi_1, z_1)$ , point  $P(\rho, \varphi, z)$  is arbitrarily selected inside solenoid,  $M$  and  $N$  are the axial coordinates of the front and rear ends of the excitation coil,  $n$  is windings per unit length,  $R_1, R_2$  are the inner and outer radius of the solenoid, respectively,  $\vec{r}$  is the position vector between the current element and point  $P$ ,  $\mu_0$  is vacuum permeability.

The magnetic induction intensity of a single-coil solenoid at the reference point  $P$  is:

$$\begin{cases} d\vec{l}_1 = (-\rho_1 \sin \varphi_1 \vec{i} + \rho_1 \cos \varphi_1 \vec{j}) d\varphi_1 \\ \vec{r}_1 = (\rho \cos \varphi - \rho_1 \cos \varphi_1) \vec{i} \\ \quad + (\rho \sin \varphi - \rho_1 \sin \varphi_1) \vec{j} + (z - z_1) \vec{k} \\ r_1 = \sqrt{\rho^2 + \rho_1^2 - 2\rho_1 \rho \cos(\varphi - \varphi_1) + (z - z_1)^2} \end{cases} \quad (1)$$

$$\vec{B}_1 = \int_{R_1}^{R_2} \int_{z_3}^{z_4} \int_0^{2\pi} \frac{n\mu_0 I}{4\pi} \frac{d\vec{l}_1 \times \vec{r}_1}{r_1^3} d\theta_1 dz_1 d\rho_1 \quad (2)$$

The sensor structure used in this system is a reverse symmetrical double-coil structure. The intensity of the magnetic field at arbitrary point  $P$  inside the sensor is simultaneously affected by the excitation coils on both sides. Analyzing the internal magnetic field distribution of a single excitation coil cannot completely represent the actual magnetic field distribution inside the sensor. Therefore, based on the mathematical model of the internal magnetic field distribution of a single coil, the internal magnetic field of the other excitation coil is theoretically analyzed and calculated. The magnetic field intensity of the other excitation coil at the reference point  $P$  is:

$$\begin{cases} d\vec{l}_2 = (-\rho_2 \sin \varphi_2 \vec{i} + \rho_2 \cos \varphi_2 \vec{j}) d\varphi_2 \\ \vec{r}_2 = (\rho \cos \varphi - \rho_2 \cos \varphi_2) \vec{i} + (\rho \sin \varphi - \rho_2 \sin \varphi_2) \vec{j} \\ \quad + (z - z_2) \vec{k} \\ r_2 = \sqrt{\rho^2 + \rho_2^2 - 2\rho_2 \rho \cos(\varphi - \varphi_2) + (z - z_2)^2} \end{cases} \quad (3)$$

$$\vec{B}_2 = \int_{R_1}^{R_2} \int_{z_5}^{z_6} \int_0^{2\pi} \frac{n\mu_0 I}{4\pi} \frac{d\vec{l}_2 \times \vec{r}_2}{r_2^3} d\theta_2 dz_2 d\rho_2 \quad (4)$$

Combining the mathematical model of the magnetic field strength of the two excitation coils at the reference point  $P$ , the magnetic field strength of the three-coil solenoid at any reference point  $P$  can be expressed as:

$$\vec{B} = \vec{B}_1 + \vec{B}_2 \quad (5)$$

This mathematical model can represent the vector sum of the magnetic field intensity of two excitation coils acting at arbitrary point in the solenoid at the same time, restore

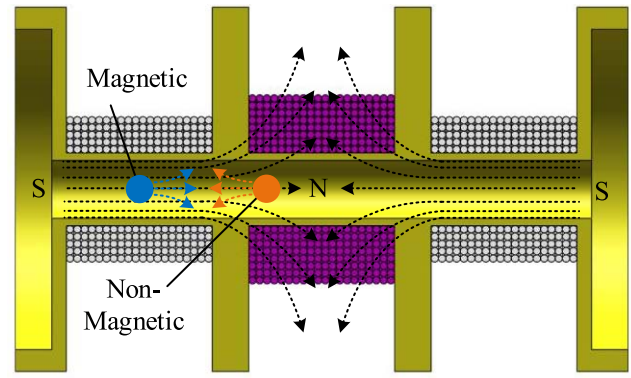


Fig. 4. Response of wear debris.

the magnetic field distribution inside the sensor under ideal conditions, and provide a theoretical basis for analyzing the relationship between the sensor signal output and the internal magnetic field.

The analysis of the internal magnetic field of the sensor includes the analysis of the magnetic field of the axis position and the non-axis position. At present, there are numerous mathematical models related to the magnetic field analysis of the internal axis position of the sensor. Based on the symmetry of the ring, there is only an axial magnetic field at any position on the axis of the current-carrying ring. In order to analyze the magnetic field distribution at the internal axis of the sensor, it is first necessary to establish a mathematical model of the magnetic field distribution in the axial direction of a single current-carrying toroidal coil. Based on this, a mathematical model of the magnetic field distribution of the internal axis of a long straight solenoid is established. Integrating the thickness of the long straight solenoid can obtain a mathematical model of the magnetic field intensity distribution on the axis of a single solenoid.

When alternating current is synchronously input to the two excitation coils of the sensor, a dynamic alternating magnetic field will be generated inside the sensor [32]. Because the magnetic field is unevenly distributed in the cross section of the sensor, the magnetic field at the inner wall of the coil is strong, while the magnetic field at the axis of the coil is weak, when the wear debris pass through the sensor along the axis, the change of inductance caused by the wear debris disturbing the magnetic field will also reduce due to the weak magnetic field on the axis.

When the wear debris in the oil pass through the sensor, it can not be guaranteed that the wear debris only pass through the sensor along the axis position. Therefore, only analyzing the distribution of the magnetic field at the axis position inside the sensor can not fully simulate the actual working conditions. In order to analyze the relationship between the signal output by the sensor and the magnetic field at any position inside the sensor. Firstly, it is necessary to analyze the strength of the magnetic field at any position in the current carrying ring, and then establish the mathematical model of the magnetic field distribution in the current carrying ring. Secondly, the current carrying ring is extended to the long straight current carrying solenoid, and the mathematical model

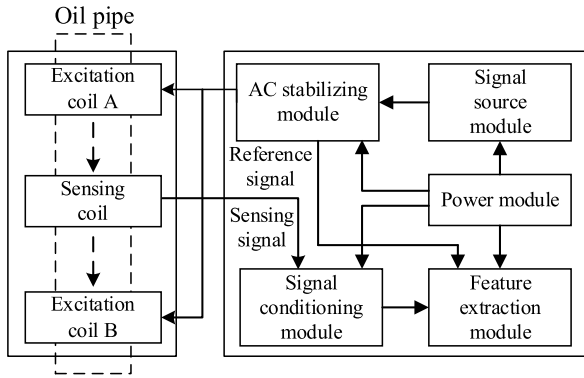


Fig. 5. System block diagram.

of magnetic field distribution in the long straight solenoid is established. Finally, based on the long direct current carrying solenoid, the mathematical model of the internal magnetic field distribution of the reverse-symmetric double-coil structure is established, which can be used as a reference for the internal magnetic field distribution of the sensor.

C. Response of Wear Debris

The response of wear debris under symmetrical magnetic excitation and magnetic variation of inductance coil caused by scattered magnetic field of wear debris are shown in Fig. 4. When alternating current is synchronously input to the two excitation coils of the sensor, a dynamic alternating magnetic field will be generated inside the sensor. The wear debris generate an induced magnetic field in the inductance coil, which is superimposed on the magnetic field of the original inductance coil to increase or decrease the inductance value of the inductance coil. When the metal wear debris pass through the dynamic alternating magnetic field, an eddy current will be formed in the metal wear debris. According to Lenz’s law, the magnetic flux generated by the eddy current will resist the change of the original magnetic flux. At the same time, the magnetic medium also has a magnetization effect in the magnetic field, causing the change of peripheral magnetic induction intensity. When ferromagnetic metal wear debris pass through the inductance coil, the relative permeability of wear debris is high, the magnetization effect of wear debris is much greater than the eddy current effect, and the magnetic induction intensity in the surrounding space will increase, which will increase the magnetic flux of the inductance coil and the equivalent inductance value. When non ferromagnetic metal wear debris pass through the inductance coil, the magnetization of the medium is not obvious, the eddy current effect of wear debris is greater than the magnetization effect, and the magnetic induction intensity in the surrounding space will decrease, which will decrease the magnetic flux of the inductance coil and the equivalent inductance value.

III. DETECTING SYSTEM

The detection system for wear debris in the oil circuit is shown in Fig. 5, including an inductive detection sensor for metal wear debris, a signal source module, an AC (alternating current) stabilizing module, a signal conditioning module,

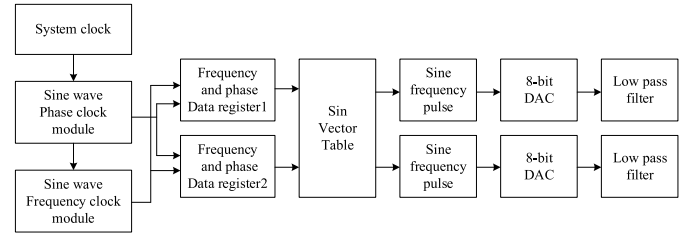


Fig. 6. Schematic diagram of excitation signal source.

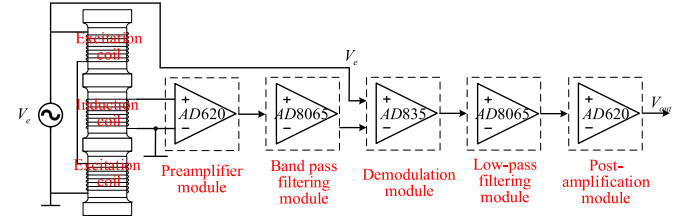


Fig. 7. Block diagram for circuit system design.

a feature extraction module, and a power supply module. The sinusoidal alternating voltage signal generated by the excitation signal source module is input to the excitation coils A and B through the AC stabilizing module to generate dynamic alternating magnetic fields with opposite polarities. At the same time, the stabilizing module outputs a reference signal to the feature extraction module. The sensing signal is input to the feature extraction module after the conditioning module improves the signal-to-noise ratio, and the signal feature extraction module [33] includes speed estimation, number estimation, and size classification. The power module provides various required voltages for each functional module.

IV. HARDWARE SYSTEM DESIGN

A. Excitation Signal Source

The characteristics of the sensing signal output by the sensor are affected by the signal source. The high-order harmonics in the excitation signal source will produce sensing signals of the same frequency on the induction coil and interfere with signal demodulation. For this purpose, the excitation signal source should have the characteristics of frequency, phase, amplitude is stable and adjustable, waveform distortion is small and so on.

DDS (Direct digital synthesizer technology) adopted by the excitation signal source is shown in Fig. 6, which is mainly composed of system clock module, frequency phase data register, sin vector table, DAC (digital to analog converter), and low-pass filter circuit. The core of DDS is the phase accumulator, the clock pulse is triggered once, the frequency phase data register automatically increases the sine vector table address index, and according to the address in the sine ROM (read only memory) table, the corresponding sine vector value is sent to the input of the 8-bit DAC. The low-pass filter is utilized to attenuate and filter out unwanted sampling components in order to output a pure sine wave signal. In addition, in order to meet the conditions of the sensing signal demodulation, the stabilizing module also needs to output an all-way excitation signal as a reference frequency signal for the demodulation module. Based on the DDS module, a sine excitation signal

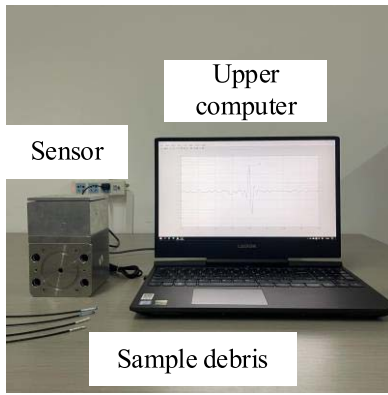


Fig. 8. Experimental system.

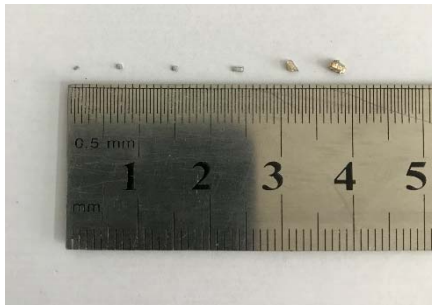


Fig. 9. Wear debris of different sizes.

with stable and adjustable frequency, phase, and amplitude can be obtained. The excitation frequency of the excitation signal source can be set according to the mathematical model of the sensing signal, the number of turns of the excitation coil, the relationship of the load, and the characteristics of the actual sensor output signal.

### B. Circuit System

The block diagram for circuit system design is shown in Fig. 7. The excitation signal source module is composed of a sine wave generator based on FPGA. The sinusoidal steady-state excitation current generated by the signal source module is input to the excitation coil to generate an excitation magnetic field. The signal conditioning module includes pre-amplification, band-pass filtering, demodulation, low-pass filtering and post-amplification modules. The sensing signal generated by the metal wear debris disturbs the magnetic field is weak and cannot meet the monitoring requirements. After the pre-amplification and band-pass filter module, the signal-to-noise ratio of the metal wear debris signal is enhanced. Aiming at the characteristics of the wear debris signal with the amplitude modulation signal, demodulation module is designed to multiply the reference signal and the sensing signal, and then the wear debris signal in the amplitude modulation signal is extracted through the low-pass filter module to complete the signal demodulation, and the wear debris characteristic signal is amplified again to facilitate the processing of the signal feature extraction module.

## V. EXPERIMENT RESULTS ANALYSIS

In order to verify the correctness and effectiveness of the above methods, The online symmetric magnetic excitation

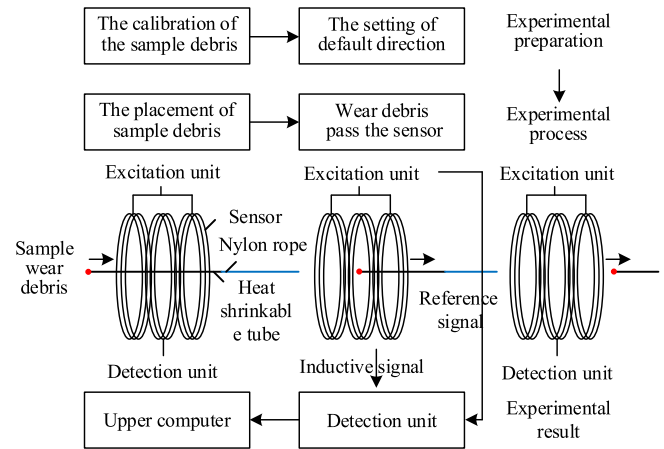


Fig. 10. Experimental system block diagram.

monitoring sensor for metal wear debris is experimentally studied. The experimental system is shown in Fig. 8, which is composed of sensor, excitation detection unit and the host computer. The excitation coil on both sides of the sensor and the central position induction coil are respectively connected with the excitation and detection unit, the excitation unit provides 8Vpp and 25 kHz sinusoidal excitation signals to drive two excitation coils to form an inverse symmetrical steady-state excitation magnetic field. The detection unit includes signal conditioning, acquisition and transmission of induced electromotive force, and the upper computer filters and displays the obtained data.

Based on the requirements of experimental environment and electromagnetic shielding, the wear debris sensor manufactured in the experiment is shown in Fig. 8. The sensor is a reverse and symmetrical three coil structure. The coils are wound with high-quality lacquered wire. The excitation coils on both sides are wound in series and reverse. The number of turns of the excitation coils on both sides is 300, and the number of turns of the induction coil at the center is 1500. The axial length of the excitation coil and the induction coil is 20 cm. The excitation coil and the induction coil are separated by a 5 cm baffle. The inner diameter of the oil pipeline is 8 mm.

The friction pair surface of mechanical equipment is usually coated with non-ferromagnetic metal coating. Therefore, in the oil pollution, there are not only conventional ferromagnetic metal wear debris, but also non-ferromagnetic metal wear debris. The experiment uses a vernier caliper to calibrate iron and copper wear debris with different particle sizes. Iron wear debris of 100  $\mu\text{m}$ , 300  $\mu\text{m}$ , 700  $\mu\text{m}$  and copper wear debris of 1000  $\mu\text{m}$ , 1300  $\mu\text{m}$ , 1500  $\mu\text{m}$  was selected as sample debris and sealed in a heat-shrinkable tube with marks. Sample wear debris are shown in Fig. 9, and the semi-physical simulation test is carried out on the produced debris samples.

The block diagram of the experimental system is shown in Fig. 10, including the preparation of each device before the experimental test and the detailed process of the experimental test.

The preparation of the experiment includes the calibration of sample debris, the setting of default direction and the placement of sample debris.

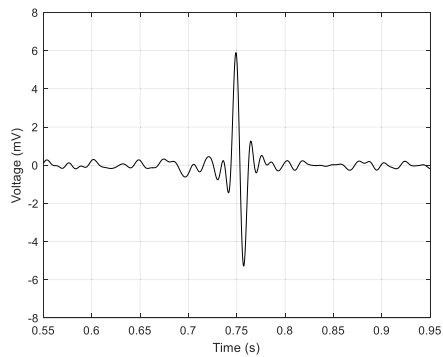


Fig. 11. 700  $\mu\text{m}$  Iron wear debris signal.

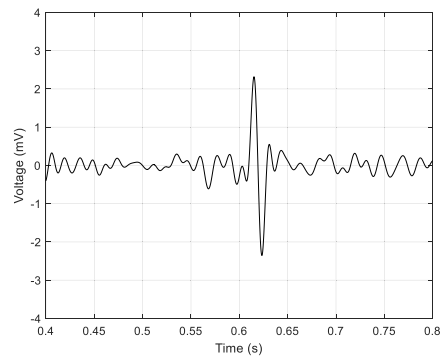


Fig. 12. 300  $\mu\text{m}$  Iron wear debris signal.

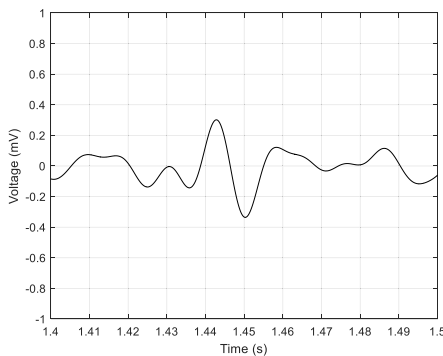


Fig. 13. 100  $\mu\text{m}$  Iron wear debris signal.

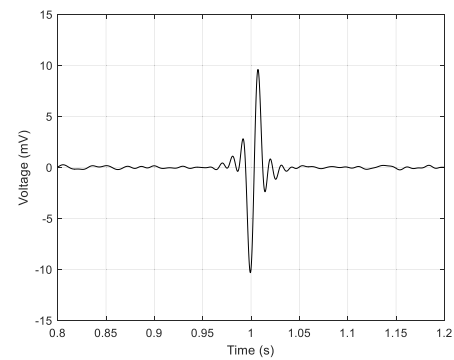


Fig. 14. 1500  $\mu\text{m}$  copper wear debris signal.

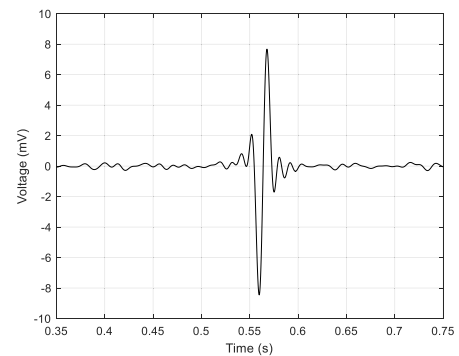


Fig. 15. 1300  $\mu\text{m}$  copper wear debris signal.

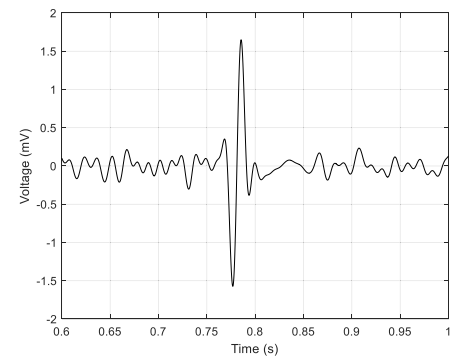


Fig. 16. 1000  $\mu\text{m}$  copper wear debris signal.

In the first step, the sample wear debris are numbered into (1) - (6) in sequence, corresponding to 100  $\mu\text{m}$  iron wear debris, 300  $\mu\text{m}$  iron wear debris, 700  $\mu\text{m}$  iron wear debris, 1000  $\mu\text{m}$  copper wear debris, 1300  $\mu\text{m}$  copper wear debris, and 1500  $\mu\text{m}$  copper wear debris.

The second step is to set the default passing direction of abrasive particles. When the wear debris pass from different sides of the sensor, the induced electromotive force changes in the opposite trend. When iron wear debris pass through the sensor, the change tendency of the induced electromotive force output by the sensor first increases and then decreases. The copper wear debris pass through the sensor, when the change tendency of the induced electromotive force output by the sensor first decreases and then increases, the system sets this direction as the default passage direction of the wear debris and marks it on the sensor housing.

The third step is to place the heat shrinkable tube encapsulating the wear debris in the sensor aperture, and

places the sample wear debris encapsulated on the top of the heat shrinkable tube 5 cm beyond the default direction of the sensor. Avoid magnetization of the wear debris due to be too close to the sensor, which will affect the detection. At the other end of the sensor, in order to prevent the human magnetic field from affecting the radial and axial magnetic field distribution inside the sensor, a non-elastic nylon rope is used to carry a heat shrinkable tube through the sensor, and the nylon rope is extended to 20 cm outside the sensor. This distance can prevent the magnetic field of the human body from affecting the detection.

In actual working conditions, the sensor is installed in the main oil circuit of the mechanical equipment. The oil entrains metal abrasive particles and passes through the sensor. The oil does not affect the output signal of the sensor due to its material characteristics. The experimental device was simplified according to the characteristics of the oil, and a semi-physical simulation experiment was conducted. The test

TABLE I  
OUTPUT SIGNAL OF FERROMAGNETIC SAMPLE WEAR DEBRIS

S.N.	Texture	Grain diameter $d / \mu\text{m}$	Peak-to-peak value $V_{pp} / \text{mV}$	Velocity $v / \text{m} \cdot \text{s}^{-1}$
1	Iron	100	0.63	5.87
2	Iron	300	5.67	5.02
3	Iron	700	11.18	5.16
4	Copper	1000	3.22	4.77
5	Copper	1300	16.12	5.16
6	Copper	1500	19.91	5.31

of wear debris shall be carried out in the order of numbers (1)-(6). After the preparation operation is completed, the sample wear debris pass through the sensor at a uniform speed. When the sample wear debris flow out of the sensor from the default direction into the other direction, the induced electromotive force caused by the change of wear debris passing through the sensor is transmitted to the upper computer through the signal conditioning module and signal characteristic module. So far, an experimental test is accomplished. When the sample wear debris pass through the detection area of the sensor at a uniform speed, it can simulate the oil carrying wear debris passing through the sensor at a certain speed under the actual working condition.

#### A. Debris Detection Sensitivity

The semi-physical simulation experiments were carried out using ferromagnetic sample debris and non-ferromagnetic sample debris of different sizes prepared in the laboratory. The output signal of ferromagnetic sample debris and non-ferromagnetic sample debris passing through the sensor is shown in Fig. 11-16.

The results of the iron wear debris experiment show that when ferromagnetic metal wear debris enter the sensor from the outside, due to the paramagnetic properties of the material, the sensing signal will first increase. When the paramagnetic metal wear debris flow from the sensor to the outside, according to Lenz's law, the induced signal will show a decreasing trend.

Tab.I, summarizes the signal characteristics of different sizes of metal wear debris when they pass through the sensor. The specific performance is the Peak-to-peak voltage amplitude and velocity of the metal wear debris.

The results of copper wear debris experiment show that when non-ferromagnetic wear debris enter the sensor from the outside, the sensing signal will decrease due to the eddy current effect of the material. When the non-ferromagnetic metal wear debris flow from the sensor to the outside, according to Lenz's law, the induced signal will increase.

The experimental results show that under the oil path experiment with aperture of 8mm and the highest flow rate of 5.87 m/s, the system can detect the smallest ferromagnetic debris grain diameter of 100  $\mu\text{m}$  and the smallest non-ferromagnetic debris grain diameter of 1000  $\mu\text{m}$ .

## VI. CONCLUSION

In this paper, an online monitoring sensor for metal wear debris with a reverse-symmetric double-coil magnetic

excitation balance magnetic field is designed, and a coupling magnetic field distribution model of reverse-symmetric double-coil magnetic excitation is established; this sensor utilizes the symmetry characteristics of the excitation magnetic field area where the detection coil is located to avoid the influence of the primary magnetic field on the response magnetic field of the metal wear debris. Through an oil path experiment with aperture of 8mm and a maximum flow rate of 5.87 m/s, effective detection of 100  $\mu\text{m}$  ferromagnetic wear debris and 1000  $\mu\text{m}$  non-ferromagnetic wear debris has been achieved. The research made in this paper provides technical support for the rapid identification and detection of hydraulic oil pollutants, which can achieve the objectives for the failure analysis of the hydraulic system and prolonging the service life of the hydraulic equipment.

## REFERENCES

- [1] X. Zhu, C. Zhong, and J. Zhe, "A high sensitivity wear debris sensor using ferrite cores for online oil condition monitoring," *Meas. Sci. Technol.*, vol. 28, no. 7, Jun. 2017, Art. no. 075102.
- [2] X. L. Zhu, C. Zhong, and J. Zhe, "Lubricating oil conditioning sensors for online machine health monitoring—A review," *Tribol. Int.*, vol. 109, pp. 473–484, Jan. 2017.
- [3] H. Wu, R. Li, N. M. Kwok, Y. Peng, T. Wu, and Z. Peng, "Restoration of low-informative image for robust debris shape measurement in on-line wear debris monitoring," *Mech. Syst. Signal Process.*, vol. 114, pp. 539–555, Jan. 2019.
- [4] A. Hamilton, A. Cleary, and F. Quai, "Development of a novel wear detection system for wind turbine gearboxes," *IEEE Sensors J.*, vol. 14, no. 7, pp. 465–473, Feb. 2014.
- [5] T. H. Loutas, D. Roulias, E. Pauly, and V. Kostopoulos, "The combined use of vibration, acoustic emission and oil debris on-line monitoring towards a more effective condition monitoring of rotating machinery," *Mech. Syst. Signal Process.*, vol. 25, no. 4, pp. 1339–1352, 2011.
- [6] M. Demori, V. Ferrari, D. Strazza, and P. Poesio, "A capacitive sensor system for the analysis of two-phase flows of oil and conductive water," *Sens. Actuators A, Phys.*, vol. 163, no. 1, pp. 172–179, 2010.
- [7] C.-T. Chiang and Y.-C. Huang, "A semicylindrical capacitive sensor with interface circuit used for flow rate measurement," *IEEE Sensors J.*, vol. 6, no. 6, pp. 1564–1570, Dec. 2006.
- [8] C. Haiden, T. Wopelka, M. Jech, F. Keplinger, and M. J. Vellekoop, "A microfluidic chip and dark-field imaging system for size measurement of metal wear particles in oil," *IEEE Sensors J.*, vol. 16, no. 15, pp. 1182–1189, Mar. 2016.
- [9] L. Du and J. Zhe, "An integrated ultrasonic-inductive pulse sensor for wear debris detection," *Smart Mater. Struct.*, vol. 22, no. 2, Feb. 2013, Art. no. 025003.
- [10] S. Murali, X. Xia, A. V. Jagtiani, J. Carletta, and J. Zhe, "Capacitive Coulter counting: Detection of metal wear particles in lubricant using a microfluidic device," *Smart Mater. Struct.*, vol. 18, no. 3, Mar. 2009, Art. no. 037001.
- [11] S. Feng, L. Yang, G. Qiu, J. Luo, R. Li, and J. Mao, "An inductive debris sensor based on a high-gradient magnetic field," *IEEE Sensors J.*, vol. 19, no. 8, pp. 2879–2886, Apr. 2019.
- [12] Y. S. Sun, H. Yang, H. B. Tong, W. Zhang, and Z. M. Zeng, "Online monitoring of aero-engine lubricant oil wear particles," *Chin. J. Sci. Instrum.*, vol. 38, no. 7, pp. 1561–1569, Jul. 2017.
- [13] L. Y. Wang, H. Zhong, L. Li, T. Chen, and J. L. Zhang, "Influence of coil spacing on output signal of oil abrasive particle detection sensor," *Lubrication Sealing*, vol. 45, no. 6, pp. 69–75, Jun. 2020.
- [14] Y. Zuo, Y. Gu, and Y. Zhang, "Design of electromagnetic sensor for metal wear particle detection in oil," *J. Eng.*, vol. 2019, no. 23, pp. 8667–8670, Oct. 2019.
- [15] C. Bai, H. Zhang, W. Wang, X. Zhao, H. Chen, and N. Zeng, "Inductive-capacitive dual-mode oil detection sensor based on magnetic nanoparticle material," *IEEE Sensors J.*, vol. 20, no. 20, pp. 12274–12281, Oct. 2020.
- [16] Y. J. Ren, G. F. Zhao, M. Qian, and Z. H. Feng, "A highly sensitive triple-coil inductive debris sensor based on an effective unbalance compensation circuit," *Meas. Sci. Technol.*, vol. 30, no. 1, Jan. 2019, Art. no. 015108.



- [17] C. Bai, H. Zhang, L. Zeng, X. Zhao, and L. Ma, "Inductive magnetic nanoparticle sensor based on microfluidic chip oil detection technology," *Micromachines*, vol. 11, no. 2, p. 183, Feb. 2020.
- [18] L. K. Liu, Z. J. Liu, S. Wu, D. Z. Liu, K. Z. Yu, and X. X. Pan, "A new method of dual-channel inductance detection based on phase division multiplexing," *Ship Eng.*, vol. 41, no. 7, pp. 80–85, Jul. 2019.
- [19] L. Ma, H. Shi, H. Zhang, G. Li, Y. Shen, and N. Zeng, "High-sensitivity distinguishing and detection method for wear debris in oil of marine machinery," *Ocean Eng.*, vol. 215, Nov. 2020, Art. no. 107452.
- [20] L. Ma, H. Zhang, W. Qiao, X. Han, L. Zeng, and H. Shi, "Oil metal debris detection sensor using ferrite core and flat channel for sensitivity improvement and high throughput," *IEEE Sensors J.*, vol. 20, no. 13, pp. 7303–7309, Jul. 2020.
- [21] H. Zhang, L. Zeng, H. Teng, and X. Zhang, "A novel on-chip impedance sensor for the detection of particle contamination in hydraulic oil," *Micromachines*, vol. 8, no. 8, p. 249, Aug. 2017.
- [22] H. Shi, H. Zhang, C. Gu, and L. Zeng, "A multi-parameter on-chip impedance sensor for the detection of particle contamination in hydraulic oil," *Sens. Actuators A, Phys.*, vol. 293, pp. 150–159, Jul. 2019.
- [23] H. P. Zhang, C. Z. Bai, G. T. Sun, and L. Zeng, "High-throughput miniature multi-parameter oil contamination detection sensor," *Opt. Precis. Eng.*, vol. 26, no. 9, pp. 2237–2245, Sep. 2018.
- [24] G. T. Sun, H. P. Zhang, C. Z. Bai, C. Z. Bai, and L. Zeng, "Design of high-precision microfluidic multi-parameter hydraulic oil detection chip," *Chin. J. Sci. Instrum.*, vol. 40, no. 2, pp. 59–66, Feb. 2019.
- [25] L. Du, X. L. Zhu, Y. Han, L. Zhao, and J. Zhe, "Improving sensitivity of an inductive pulse sensor for detection of metallic wear debris in lubricants using parallel LC resonance method," *Meas. Sci. Technol.*, vol. 24, no. 7, Jun. 2013, Art. no. 075106.
- [26] X. L. Zhu, L. Du, and J. Zhe, "A 3×3 wear debris sensor array for real time lubricant oil conditioning monitoring using synchronized sampling," *Mech. Syst. Signal Process.*, vol. 83, pp. 296–304, Jan. 2017.
- [27] Y. J. Ren, W. Li, G. F. Zhao, and Z. H. Feng, "Inductive debris sensor using one energizing coil with multiple sensing coils for sensitivity improvement and high throughput," *Tribol. Int.*, vol. 128, pp. 96–103, Dec. 2018.
- [28] H. Xiao, X. Y. Wang, H. C. Li, J. F. Luo, and S. Feng, "An inductive debris sensor for a large-diameter lubricating oil circuit based on a high-gradient magnetic field," *Appl. Sci.*, vol. 9, no. 8, p. 1546, Apr. 2019.
- [29] H. Xiao, W. Zhou, J. F. F. Luo Tan, and S. Feng, "A high-gradient static magnetic field induction full flow wear particle monitoring sensor," *Chin. J. Sci. Instrum.*, vol. 41, no. 6, pp. 10–18, Jun. 2020.
- [30] B. Liu, F. Zhang, D. Li, and J. Yang, "Research on the influence of excitation frequency on the sensitivity in metal debris detection with inductor sensor," *Adv. Mech. Eng.*, vol. 6, Jan. 2014, Art. no. 790615.
- [31] H. Haimovich, D. Marelli, and D. Sarlinga, "A signal processing method for metal detection sensitivity improvement in balance-coil metal detectors for food products," in *Proc. IEEE Int. Conf. Ind. Technol. (ICIT)*, Feb. 2020, pp. 645–651.
- [32] C. S. Zheng, M. Li, Z. Gao, and T. Chen, "Method for extracting electromotive force of inductive wear sensor," *J. Vib., Meas. Diagnosis*, vol. 36, no. 1, pp. 36–41, Feb. 2016.
- [33] Y. Gu, S. Liu, Y. Zuo, and L. Wang, "Research on the excitation method of symmetrical spiral online detecting sensor of metal debris," *J. Eng.*, vol. 2019, no. 23, pp. 8760–8764, Dec. 2019.



**Wenbin Bai** born in Jinzhong, Shanxi, China, in 1997. He received the bachelor's degree from the Yancheng Institute of Technology in 2019. He is currently pursuing the master's degree in information and communication engineering with the North University of China. His research interests include oil monitoring and circuit system design.



**Yuan Li** received the B.S. degree in communication engineering and the M.S. degree in signal and information processing technology from the Taiyuan University of Technology, China, in 2003 and 2006, respectively, and the Ph.D. degree in weapon science and technology from the North University of China, China, in 2014. She is currently an Associate Professor and a Master Supervisor with the School of Signal and Information Processing, North University of China. Her main research interests include signal and information processing, optical device, and sensor.



**Shichao Zhou** was born in Yuncheng, Shanxi, China, in 1997. He received the bachelor's degree in information countermeasures technology from the North University of China, China, in 2020, where he is currently pursuing the master's degree in information and communication engineering. His research direction is information detection and processing.



**Kai Li** (Member, IEEE) received the Ph.D. degree in signal and information processing from the North University of China, China, in 2017. He is currently an Associate Professor with the School of Signal and Information Processing, North University of China. Since 2010, he has been involved in magnetic sensor design on integrated transceivers, and holds five patents. His current research interests include electromagnetics and sensor.



**Peng Wen** was born in Datong, Shanxi, China, in 1997. He received the bachelor's degree in information countermeasures technology from the North University of China, China, in 2020, where he is currently pursuing the master's degree in information and communication engineering. His research direction is information detection and processing.